# Statistical Evaluation of Laser Energy Density Effect on Mechanical Properties of Polyamide Parts Manufactured by Selective Laser Sintering

**V. E. Beal,[1] R. A. Paggi,[2] G. V. Salmoria,[2] A. Lago[3]**

[1]*SENAI-CIMATEC, Serviço Nacional de Aprendizagem Industrial, FIEB, Salvador, BA, Brazil*
[2]*CIMJECT, Depto de Engenharia Mecânica, Universidade Federal de Santa Catarina, Florianópolis, SC, Brazil*
[3]*LABMAT, Depto de Engenharia Mecânica, Universidade Federal de Santa Catarina, Florianópolis, SC, Brazil*

Received 6 April 2008; accepted 24 February 2009
DOI 10.1002/app.30329
Published online 1 May 2009 in Wiley InterScience (www.interscience.wiley.com).

**ABSTRACT:** Selective laser sintering (SLS) is a rapid manufacturing technology that builds layer-by-layer solid object from particulate materials. Nowadays there are materials that are used to produce prototypes and end-user parts. Powders might be made from metals, ceramics, polymers, and composites. The union or fusion of the particles is made by the energy provided by a heated environment and a laser beam. Parts are built based on data extracted from its CAD design. The process has many variables that directly affect the mechanical properties of the parts. One important and direct processing parameter is laser energy density. This work evaluated the effect of the variation of the energy density in the mechanical properties of a polymeric material by changing laser beam speed and average power. The analyzed variables were stress at 10% of elongation, flexural modulus, and density of the samples built with polyamide 2200 (PA2200-EOSINT) using a $CO_2$ laser (10 W). Specimens obtained by combination of different laser powers (2.7, 3.4, and 4.1 W) and laser scan speeds (39.0, 44.5, and 50.0 mm/s) were submitted to flexural tests. Additionally, volumetric density was calculated with mass and physical dimensions of specimens, and micrograph were taken using scanning electron microscope to analyze the changes of the sintering degree. The results indicated that laser power had more influence over density and mechanical properties than scan speed. The microstructures presented good correlation with the statistical results. © 2009 Wiley Periodicals, Inc. J Appl Polym Sci 113: 2910–2919, 2009

**Key words:** selective laser sintering; polyamide; processing parameters; rapid manufacturing; prototyping

## INTRODUCTION

Product designers and engineers have been using rapid prototyping (RP) technologies to perform evaluations during product development cycle. These technologies provide quick prototypes with different types of materials, accuracy, and costs depending on the chosen technology and subject of evaluation. Technologies and materials have been constantly improved and it is possible to produce parts directly from CAD data without the need of tooling or setup.[1] Additionally, RP machines can be used to produce tools such as injection molds that might be able to produce from few dozens to 10,000 parts (rapid tooling, RT). Also, rapid manufacturing (RM) is the use of RP machines to build durable end-user parts.

An important and popular RP technology is selective laser sintering (SLS), which is able to build parts in polymers, ceramics, and metals. SLS process uses a laser that sinters selectively a thin layer of powder spread over a moving platform. Each time a layer is finished, the platform is lowered and a new layer of powder is spread over the previously built layer. A computer directs the laser scanning mirrors over the powder layer, sintering and attaching a new layer of the part. The process continues until the part is complete and few postprocessing steps are required to cool down and clean the unsintered powder.[2]

During the SLS process, it is necessary to control different parameters to obtain successful parts depending on the type of material under processing. For instance, the laser used to sinter metals is different from the laser used to sinter ceramics and polymers as the wavelength must interact differently with the atoms, crystalline structure, or polymer chain. In the case of polymers, the $CO_2$ infrared laser is commonly used in the continuous mode and the main processing variables are as follows: the average laser power, the scan speed, and the overlap of the scan vectors and spot diameter. These variables determined the amount of energy directed to the powder over the platform. Considering only one bead of the laser scan vector, the energy density can be calculated by eq. (1) as follows:

*Correspondence to:* V. E. Beal (valtereb@fieb.org.br).
Contract grant sponsors: FAPESC, FINEP, CNPq, CAPES.

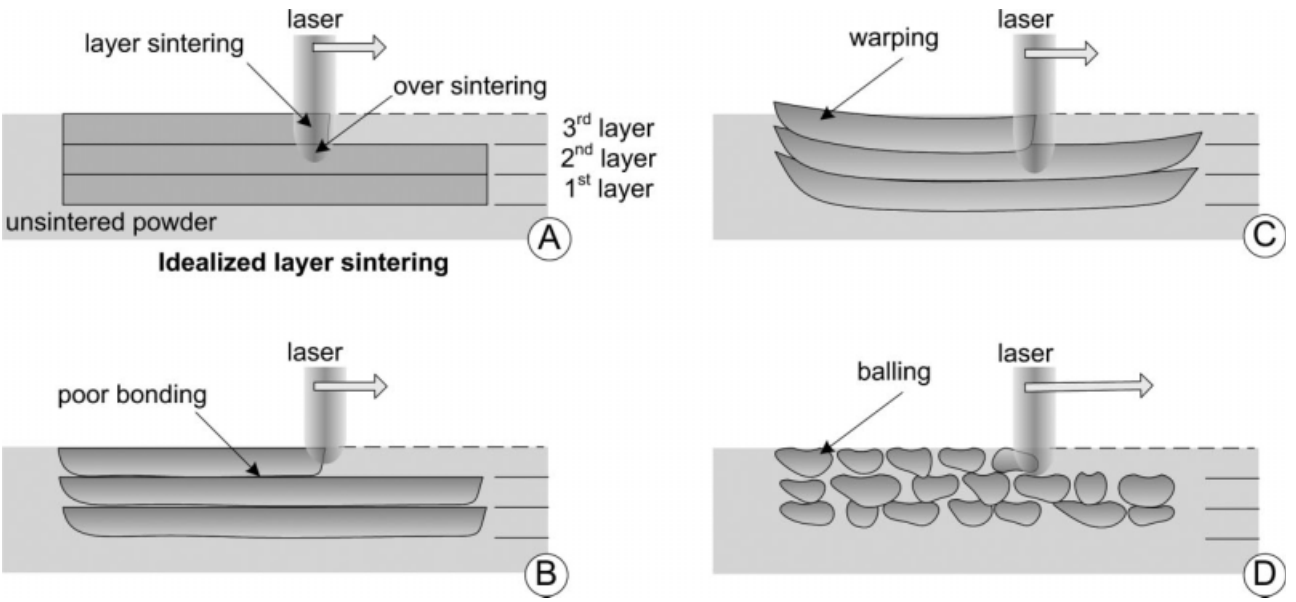


**Figure 1** Different effects of the laser energy density variation.

$$\rho_e = P/(v \cdot d) \quad (1)$$

where $\rho_e$ (J/mm$^2$) is the laser energy density, $P$ (W) is the laser power, $v$ (mm/s) is the scan speed, and $d$ is the spot diameter (mm) over the powder surface.[3]

According to Gusarov et al.,[4] the laser beam heat transfer is strongly affected by the formation and growth of necks between powder particles during sintering. The heat transfer of the powder particles is complex and the contact conductivity increases as sintering occurs. The effective thermal conductivity is proportional to the linear dimension of generated contacts. Therefore, SLS process is a three-dimensional unsteady heat transfer problem and powder changes from solid phase to liquid phase and then returns to the solid phase. These phase changes are accompanied by both absorption and release of thermal energy.[5] Thus, the powder characteristics and particles size are very important factors to obtain the desired sintering degree, accuracy, and stability. Kosolov et al.[6] evaluated different deposition techniques and concluded that classical deposition method (using a sliding hopper with blades) is successful with a particle size range of 20–100 μm.

Although the laser is precise, the energy density is high, which makes it difficult to control the process if performed in nonheated and nonprotective environment as thermal gradients are too high. To overcome this problem in processing semicrystalline polymer, such as polyamide, the chamber is heated few degrees below the melting point and nitrogen is used as the shield gas.[7] Ideally, the laser should only sinter the unsintered powder of the new layer and bond it to the previous layer built as seen in Figure 1(A). According to Hardro et al.,[8] if the energy density is low (insufficient laser power or too fast scan speed), it can cause poor bonding between the layers making them weak and easy to delaminate [Fig. 1(B)]. In case of excessive power or too slow speed it might cause the layers to warp [Fig. 1(C)]. Warping make deformed parts and in critical cases it blocks the recoat of new layers and interrupts the process. Another consequence of nonadjusted combination of properties might cause balling presented in Figure 1(D). Balling is characterized by isolated amounts of fused powders and it might happen in case of high power and too fast scan speed.

Furthermore, the energy density affects the resultant microstructure of the sintered polymer. The higher the energy and lower the porosity, higher the shrinkage and higher mechanical properties might be achieved (Fig. 2). Nevertheless, as commented previously, too high energy might cause undesirable results during the part built and might degrade the polymer decreasing its properties. Also, the amount of energy incident over the powder changes the cooling rate and so the crystallinity degree. According to Zarringhalam et al., [9] it is essential that polymers to be processed by SLS should have their melt temperature higher than the crystallization temperature so that crystallization can be delayed and reduced during the building process to allow layers to bond and forming homogenous microstructure.

Because it is important for RM to control the mechanical properties, it is necessary to control the processing parameters based on the machine characteristics and powder properties. So, parts built by SLS technology should achieve mechanical pro-

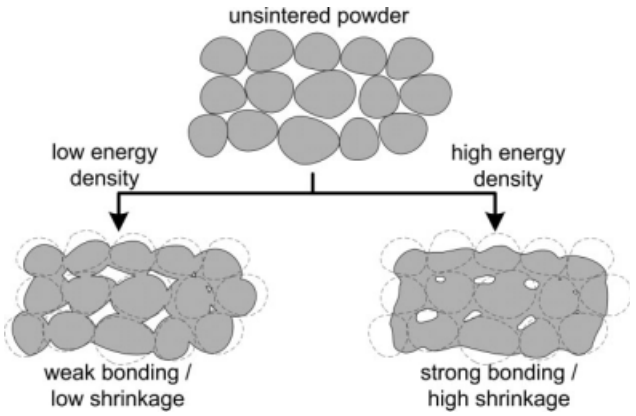


**Figure 2** The effects of energy density variation over powder particles bonding.

perties compared with parts obtained by injection molding. In addition, they must present advantages beyond the free-form fabrication. For metals, polymers, and glasses, laser sintering has produced many materials/components with unusual microstructures and properties, which cannot be obtained using other manufacturing technologies. Ch'ng and Pan[10] studied the problem of cosintering between two cylindrical particles of different sizes using numerical tools. Their work consisted on understanding how the change in the particle arrangement affected the way in which particles sinter and the size of particles interplay between the mechanisms of matter redistribution. The authors observed that a small particle can grow at the expense of its larger neighbors. According to the authors, there are two conditions for this to occur. The first reason is because the particles have to be sufficiently small for surface diffusion to dominate the process rather than grain-boundary migration, which typically requires nanosized particles. The second condition occurs when the small particle is placed between two larger neighbors.

In this work, the variation of the laser energy density was studied to observe and characterize the mechanical properties based on the input variables. Different levels of laser power and scan speed were combined and their individual influence over some properties of polyamide were analyzed. Using design of experiments methodology, experiments were performed to determine the better combination of laser power and beam speed. The objectives were to increase the material density and analyze the flexural modulus and stress at 10% elongation.

## MATERIALS AND METHODS

The experiments were carried out by manufacturing small slabs of the subject material with approximate dimensions of 35.0 mm × 5.0 mm × 1.45 mm. The polymer used in this study was fine polyamide PA2200 from EOS with an average grain size obtained by laser diffraction of 60 μm. The PA2200 melting temperature was 177°C obtained by differential scanning calorimetry analysis (DSC).[11] The scanning strategy was to alternate the **X** and **Y** scanning vectors between subsequent layers.

The specimens were manufactured using a prototype SLS machine, schematically presented in Figure 3. To improve the accuracy and avoid distortion during the building process, infrared lamps and heaters were used to keep the temperature of the unsintered powder and sintered layers around 140°C. A sliding hopper was used to spread powder over the platform to add new layers. Two mirrors controlled the scan over the surface of the powder bed, selectively sintering the programmed layer. A dioxide carbon laser unit was used with a nominal power of 10 W. The lenses provided a laser beam focus of 250 μm, and the machine was capable of producing parts with average layer thickness of 200 μm. The scan-spacing strategy used in the experiments maintained an overlap of 125 μm between each scan vector.

The selection of the laser and speed range was based on previous results presented in Ref. 12. In this work, exploratory experiments were performed to achieve stability during the process and final parts. So, the experiment was designed to find the best combination between laser power of 2.7, 3.4, and 4.1 W and scan speeds of 39.0, 44.5, and 50.0 mm/s. A factorial multilevel design was planned to evaluate the inputs: power and speed; and outputs: density, stress and 10% strain, and flexural modulus. It was randomized and a summary of the experiment is shown in Table I.

The volumetric density was calculated based on the measured mass and dimensions of the

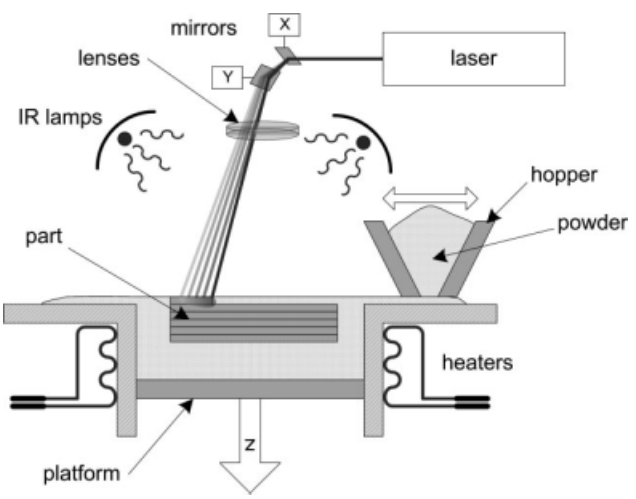


**Figure 3** Schematic representation of the prototype SLS machine used in the experiments.

**TABLE I**
**Statistical Summary of the Experiment**

| Class of project | | | | Factorial multilevel |
|---|---|---|---|---|
| Experimental factors | | | | 2 |
| Responses | | | | 3 |
| Number of runs | | | | 36 |
| Degrees of freedom | | | | 27 |
| Randomized | | | | Yes |
| Confidence interval | | | | 95% |
| Input factors | Laser power | Low | 2.7 | W |
| | | Mid | 3.4 | |
| | | High | 4.1 | |
| | Scan speed | Low | 39.0 | mm/s |
| | | Mid | 44.5 | |
| | | High | 50.0 | |
| Output factors | Density | | | $g/cm^3$ |
| | Flexural modulus | | | MPa |
| | Stress at 10% | | | MPa |

specimens. The images of the microstructures were obtained using a scanning electronic microscope (SEM), Phillips XL30, to evaluate the surfaces and the flexural fracture surface of the samples. Moreover, dynamic mechanical analysis equipment (DMA Q800, TA Instruments) was used to obtain the mechanical properties. To perform the single cantilever test, the applied force had a rate of 2 N/min, and all samples were tested at 30°C.

## RESULTS AND DISCUSSION

Thirty-six specimens were built as planned by the statistical experiment. In Figure 4, four specimens are shown and no visible difference in surface finishing, color, or geometry form was noticed.

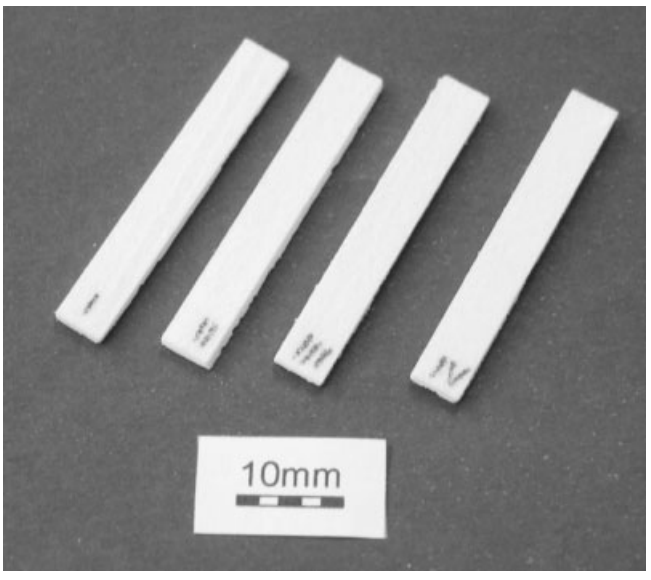


**Figure 4** Polyamide specimens obtained during the experiments.

**TABLE II**
**ANOVA for Density**

| Source | Sum of squares | $D_f$ | Mean square | *F*-ratio | *P*-value |
|---|---|---|---|---|---|
| A: Laser power | 0.058115 | 1 | 0.058115 | 90.59 | 0.0000 |
| B: Scan speed | 0.0567454 | 1 | 0.0567454 | 88.45 | 0.0000 |
| AA | 0.0242367 | 1 | 0.0242367 | 37.78 | 0.0000 |
| AB | 0.000150063 | 1 | 0.000150063 | 0.23 | 0.6322 |
| BB | 0.00553001 | 1 | 0.00553001 | 8.62 | 0.0063 |
| Total error | 0.0192464 | 30 | 0.000641546 | | |

### Analysis of variance

Tables II–IV show the analysis of variance (ANOVA) for each output variable measured in the experiment. The sources that had *P*-value below 0.05 had strong influence over the result. The greater the *F*-value, the greater is the influence and relevance of the source factor. All the ANOVA was performed at 95% confidence interval.

To summarize the previously presented results, Table V shows the significant and predominant factors for each result. The predominant factor indicated in the table was the strongest effect over the results. It can be seen that laser power had greater impact on density and stress at 10%. The beam scan speed was the predominant factor for the flexural modulus; however, there was almost no difference between the scan speed and laser power when comparing the *F*-ratio values. In this way, laser power was considered as a significant factor together with scan speed.

### Response surfaces

To better understand the influences of each factor, the regression coefficients of the equations that represent the phenomena were obtained. The equations were used to plot the estimated response surfaces of the results based on the interaction between laser power and scan speed.

In Figure 5, the estimated response surface for the volumetric density is presented. The best optimized combination to achieve higher density (0.732 $g/cm^3$) was at lower scan speeds (39.5 mm/s) and relative

**TABLE III**
**ANOVA for Flexural Modulus**

| Source | Sum of squares | $D_f$ | Mean square | *F*-ratio | *P*-value |
|---|---|---|---|---|---|
| A: Laser power | 38929.8 | 1 | 38929.8 | 72.92 | 0.0000 |
| B: Scan speed | 41275.9 | 1 | 41275.9 | 77.31 | 0.0000 |
| AA | 27753.7 | 1 | 27753.7 | 51.98 | 0.0000 |
| AB | 1413.76 | 1 | 1413.76 | 2.65 | 0.1141 |
| BB | 183.361 | 1 | 183.361 | 0.34 | 0.5622 |
| Total error | 16017.1 | 30 | 533.902 | | |

**TABLE IV**
**ANOVA for Stress at 10%**

| Source | Sum of squares | $D_f$ | Mean square | *F*-ratio | *P*-value |
|---|---|---|---|---|---|
| A: Laser power | 832.728 | 1 | 832.728 | 20.19 | 0.0001 |
| B: Scan speed | 37.575 | 1 | 37.575 | 0.91 | 0.3475 |
| AA | 275.069 | 1 | 275.069 | 6.67 | 0.0149 |
| AB | 17.1603 | 1 | 17.1603 | 0.42 | 0.5238 |
| BB | 223.767 | 1 | 223.767 | 5.42 | 0.0268 |
| Total error | 1237.46 | 30 | 41.2486 | | |

high laser power (3.72 W) demonstrated by the peak in the surface in Figure 5. In this peak, the energy density was 0.37 J/mm$^2$ and, as previously seen, the scan speed had less influence on the results than the laser power. In Ref. [13], the authors also agreed that the laser power and powder bed temperature had more influence over the laser sintering results than the laser scan speed in the manufacturing of fully dense parts.

Although the high laser power caused higher density, it may also cause the material deterioration. As the machine was not capable of using an inert gas inside its chamber, this might become critical affecting other mechanical properties. On the other hand, Ho et al.[14] affirmed that density reduction is probably a result of polymer degradation and expansion of the voids by trapped gases. For this reason, the tendency of decreasing density at higher energy densities in the surface of Figure 5 is justified.

The estimated response surface for the flexural modulus is presented in Figure 6. This resultant surface shows that scan speed had strong influence over the results. It was acquired that a speed of 39.0 mm/s and laser power of 3.69 W would produce stiffer parts (361.7 MPa). For this combination of speed and power, the energy density was 0.37 J/mm$^2$. This influence might be related to the time exposure of the material to the heat source that might have affected the kinematics of the laser sintering process. The response surface indicates that at lower speeds the material might become more rigid. Although lower speeds had caused an increment in the flexural modulus, the increment of the laser power had a slight reduction. The estimated response surface showed that to achieve higher flexural modulus, a combination of lower scan speed and moderate to high laser power have to be further studied.

**TABLE V**
**Summary of Analysis of Variance**

| Properties | Significant factors | Predominant factor |
|---|---|---|
| Density | A: Laser power<br>B: Scan speed<br>AA<br>BB | Laser power |
| Flexural modulus | A: Laser Power<br>B: Scan speed<br>AA | Scan speed |
| Stress at 10% | A: Laser power<br>AA<br>BB | Laser power |

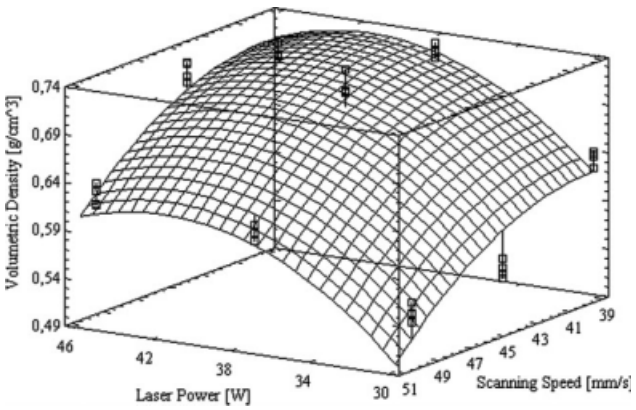


**Figure 5** Estimated response surface for volumetric density.

The stress at 10% strain response surface had similar behavior to the density results as presented in Figure 7. The optimum value of stress, 50.2 MPa, was obtained by a combination of scan speed of 44.0 mm/s and laser power of 3.78 W resulting in an energy density of 0.34 J/mm$^2$. As discussed previously, the deterioration of powder caused by broke of polymer chains may decrease the mechanical properties of the material. Internal structure of porosity inherently present on sintered parts certainly has contribution on the dispersion of results and their behavior.

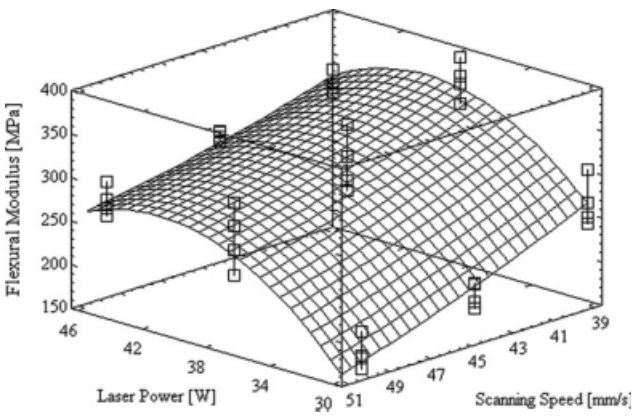


**Figure 6** Estimated response surface for flexural modulus.

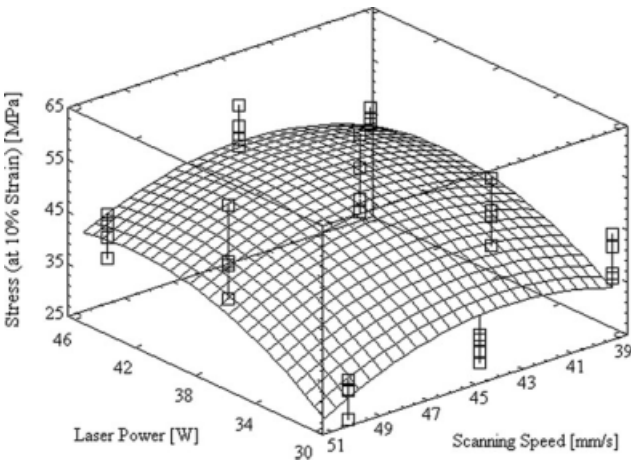


**Figure 7** Estimated response surface for stress at 10% strain.

### Microstructure

Sintering behavior between polyamide powder and laser beam was investigated by SEM micrographs. The micrographs taken are shown in Figure 8, where specimens' top surface and fracture are presented. The examination of microstructure can explain the mechanical properties obtained. Analyzing the micrographs it is possible to observe that as the energy density increased, the higher was the sintering degree observed by the increase of melted particles. Figure 8 shows the micrographs for fixed scan speed of 50 mm/s. The low energy density provided by low laser power condition was favorable to the appearance of defects and voids. According to Caulfield et al.,[7] at the lowest energy density level, the powder particles within the parts were loosely bound and the majority of particles could be recognized individually, which can be observed by the micrographs presented. By incrementing laser power, better fusion between particles forming regions with continuous phase (fused) in the surface becomes visible. The fractures also showed larger necks with 3.4 W and regions of brittle fracture using 4.1 W. Therefore, the continuous phase obtained with higher laser power improved the density and strength of parts because it reduced the

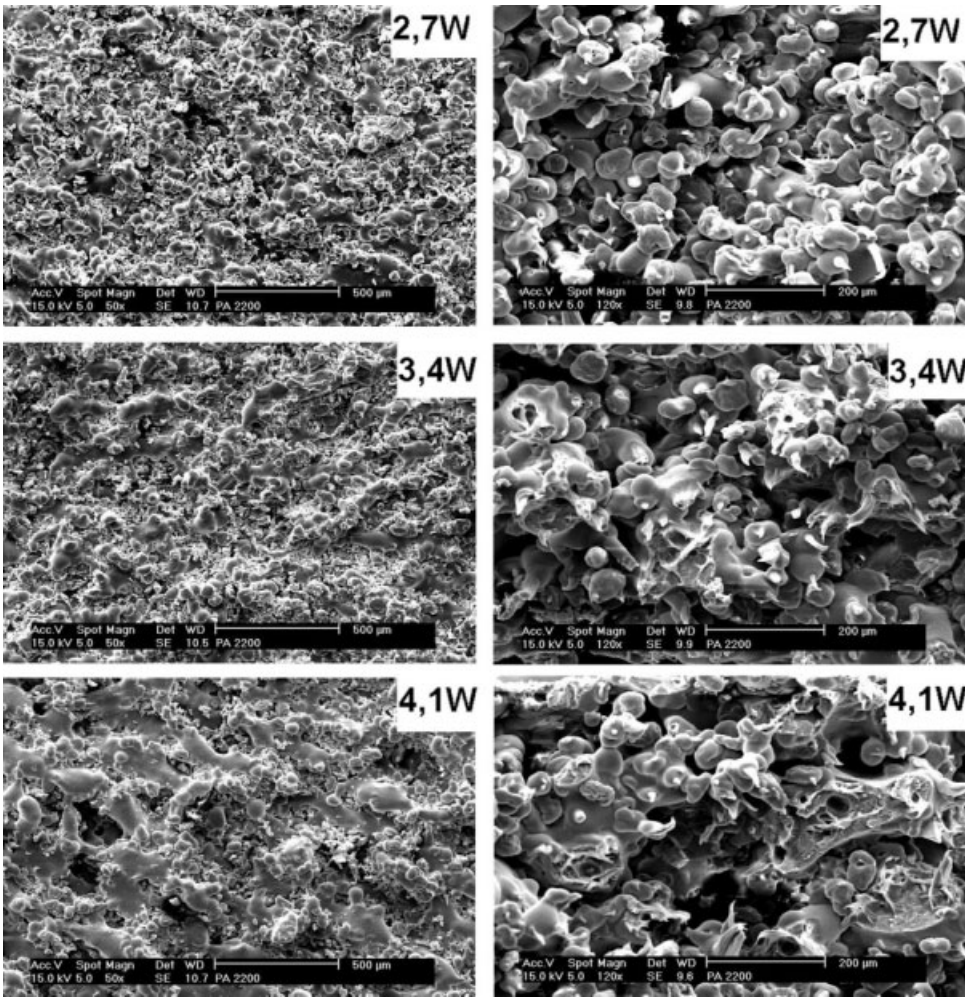


**Figure 8** Surface (left) and fracture (right) SEM micrographs for scan speed of 50.0 mm/s.

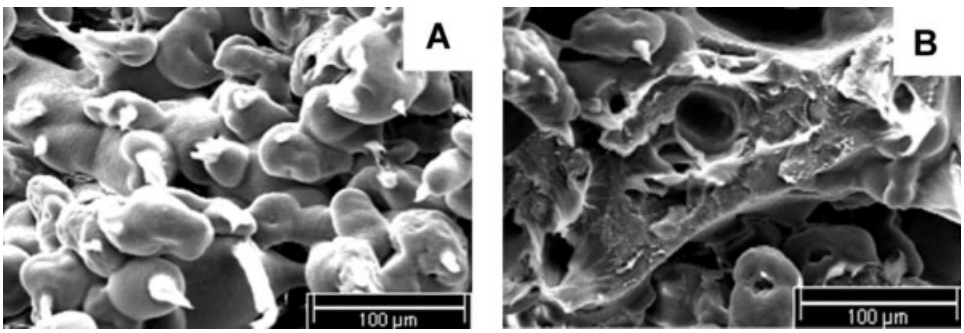


**Figure 9** SEM micrographs of low-energy sintered (a) and high-energy sintered necks (b).

pores and defects in the structure of the material. In the specimen's fracture surface built with 2.7 W, some yielded points of contact with reduced fractured area can be seen, which might lead to higher elongation at break.

Sintered specimens with higher laser power presented a rough surface caused by high shrinkage of the fused material but defects in the low energy densities were detected as well. The surface crack with low energy density presented small fractured necks as seen in Figure 9(A). This microstructure might produce more toughened/bendable parts. On the other hand, microstructures obtained with high energy density, as presented in Figure 9(B), with strongly sintered necks might have higher elongation modulus and ultimate tensile strength.

The previously presented results were based on 50 mm/s scan speed, and in the results with lower

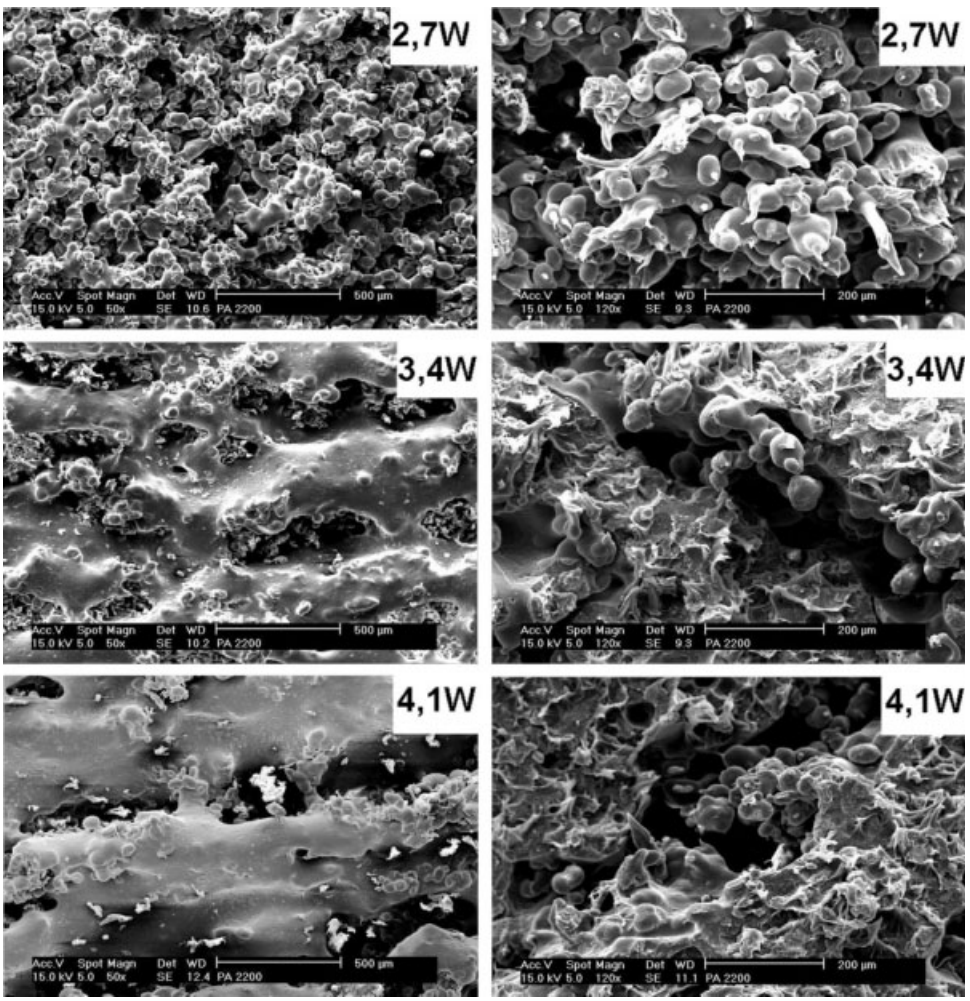


**Figure 10** Surface (left) and fracture (right) SEM micrographs for scan speed of 44.5 mm/s.

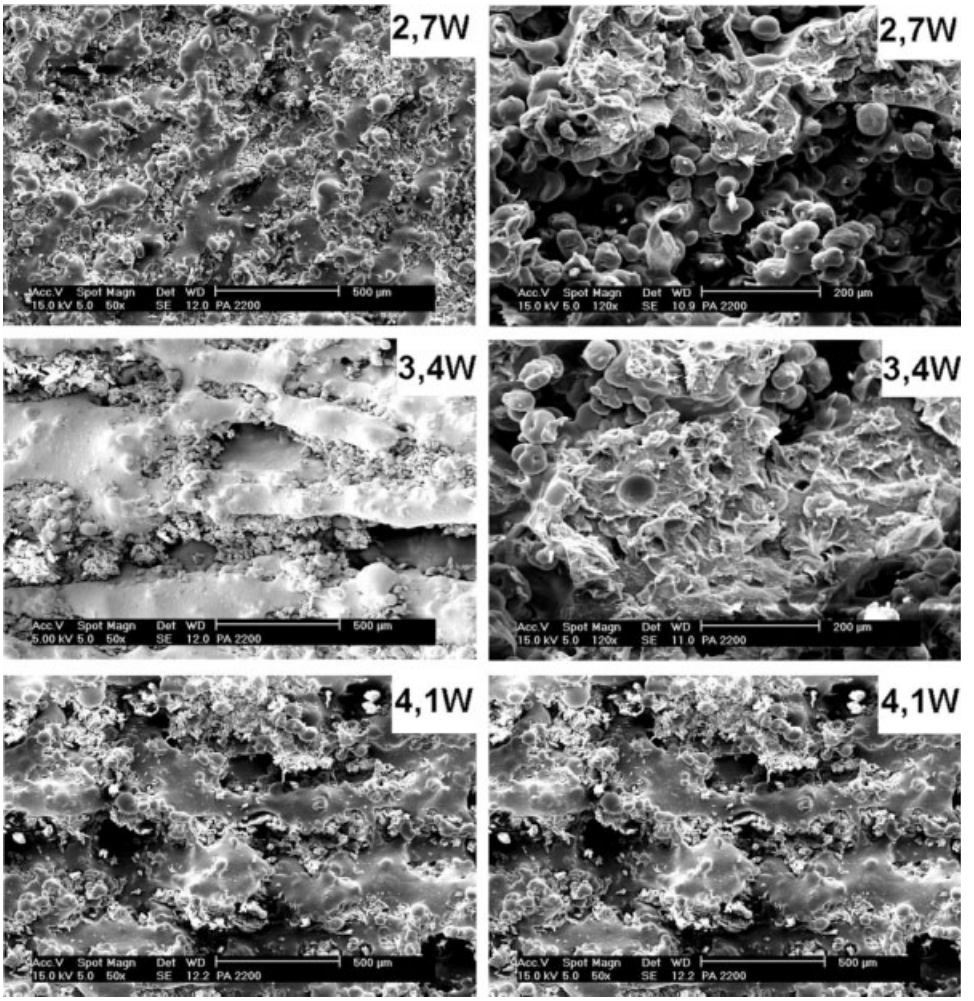


**Figure 11** Surface (left) and fracture (right) SEM micrographs for scan speed of 39.0 mm/s.

scan speed, the energy density supplied to material was increased. Aspects of surface and fracture for 44.5 mm/s are shown in Figure 10. Results obtained by ANOVA showed that laser power is the predominant factor under density and strength of parts, and in accordance with micrographs analysis it shows a progressive increase of fused regions that explain higher density. The strength of parts is verified in function of large resistant transversal area of solid material obtained in the specimens as the melted regions observed were larger.

Figure 11 shows the micrographs of specimens sintered with the lower tested scan speed (39.0 mm/s) and the same variation on laser power. In the images of the surfaces obtained with 3.7 and 4.1 W, the effect of excessive shrinkage identified by large fused and/or poorly connected regions becomes clear. These poor connection regions could be identified as the middle distance between laser beam scanning vectors. One cause for the pronounced shrinkage in the laser beam paths might be the chamber temperature supplied by the prototype machine used in the experiment. With higher temperature, the shrinkage should be less excessive allowing more homogeneous microstructures. Also, the adjustments in the scan vectors must be performed to increase or decrease the overlap of the vectors.

In the micrographs of the fracture surfaces presented in Figure 11, holes caused by detaching of unsintered particles can be seen. This fact reports existence of loose particles or pores caused by humidity/gases inside the part, which might lead to possible spot for crack initiation.

According to the statistical analysis, the laser scan speed was the predominant factor for the flexural modulus results and voids must be avoided into the microstructure to achieve higher values. As a consequence, the comparison of micrographs with the ANOVA results shows that more dense areas obtained for laser powers of 3.4 and 4.1 W and scan speed of 44.5 mm/s (Fig. 10) had the best values of the flexural modulus. Comparing the responses of mechanical properties with the micrographs

analysis, it showed good correlation with the statistical test selected for the experiment. The different microstructures obtained were more sensitive to the laser variation than the scanning speed.

Analyzing the images presented in Figures 9–11, it could be observed that all laser sintering samples had an important amount of porosity. This created noise between the correlations of mechanical properties and processing parameters. Ajoku et al.[15] developed a study comparing injection-molded and laser sintering Nylon-12 parts. The modulus of laser sintering parts was 10% less than the injection-molded parts, and the difference was explained by porosity. However, in the same study, the laser-sintered part had higher strength value than those obtained by injection molding.

### Multiple response optimizations

SLS parts can be used in different applications that might require different mechanical properties for the same material as there are few materials available besides the advances in last 10 years. For this reason, multiple response optimizations could be used to achieve different mechanical properties that might tailor the material to the part application. To resume, multiple response optimization is the overlapping of the curves from the estimated response surfaces obtained for each of the previously presented results (Figs. 5–7). For the most usual applications for RM or RP, dense parts with maximum flexural modulus and stress are required. This case is shown in Figure 12, where the peak of the curve is the best combination of scan speed and laser power to obtain dense, stiff, and strong parts. The scale of desirability is a number, from 0 to 1, that represents how far or close is the optimization from the desired combination of the two response variables.

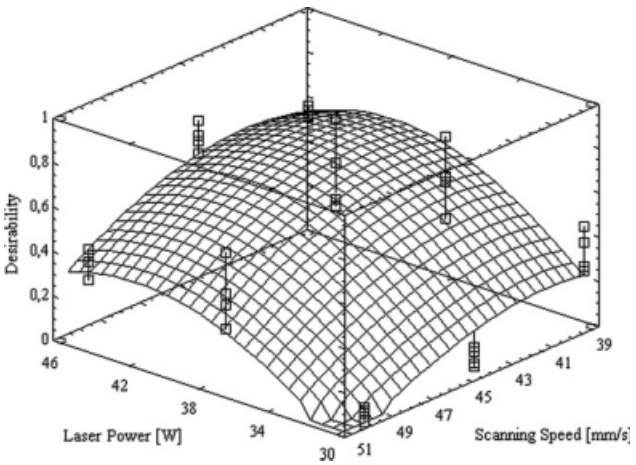


**Figure 12** Estimated desirability surface for strong, stiff, and dense material.

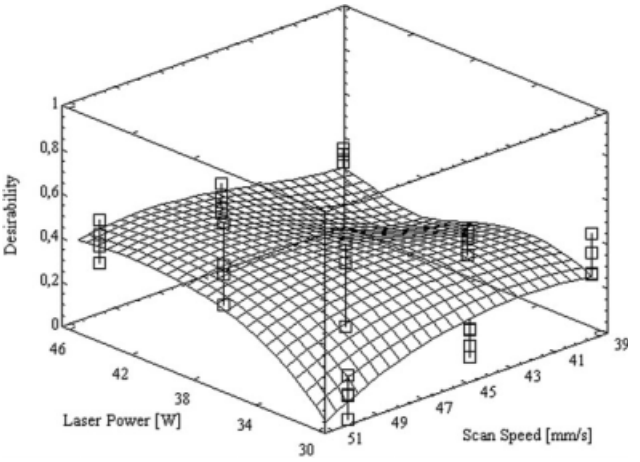


**Figure 13** Estimated desirability surface for minimum density (porous material) with maximum stress and flexural modulus properties.

Nevertheless, other applications might not require dense parts. As a manner of fact, applications such as tissue engineering and time-controlled drug delivery capsules could require both dense and porous materials in the same part.[16,17] For this kind of application, the optimization is represented by the estimated response surface shown in Figure 13. The complex shape was the result of the difficulty for obtaining maximized stress and flexural modulus with low density. As the low density was obtained by higher amount of pores inside the material, it was difficult to maximize the other two properties as the internal porous structure reflects in the section area of the samples.

In Table VI the summary of the multiple response optimizations is presented. In the case of stiff, strong, and dense parts, the desirability achieved was 0.69. On the other hand, the higher desirability

**TABLE VI**
**Summary of the Multiple Response Optimizations**

| | Target[a] | Target[b] |
|---|---|---|
| Factor | Value | |
| Laser power (W) | 3.71 | 3.82 |
| Scan speed (mm/s) | 41.9 | 48.9 |
| Energy density[c] (J/mm$^2$) | 0.35 | 0.31 |
| Response | Optimum value | |
| Density (g/cm$^3$) | 0.728 | 0.656 |
| Flexural modulus (MPa) | 337.1 | 289.7 |
| Stress at 10% (MPa) | 49.3 | 46.2 |
| Desirability | 0.69 | 0.43 |

[a] The target includes the following: maximum density, maximum flexural modulus, and maximum stress.
[b] The target includes the following: minimum density, maximum flexural modulus, and maximum stress.
[c] Calculated.

for strong and stiff but porous parts was 0.43. Comparing both cases, the scan speed was the factor that had higher degree of changes. Care must be taken to not analyze the multiple response optimizations isolated from the ANOVA of each isolated response.

## CONCLUSIONS

The objective of this work was to study the effect of the laser power and scan speed over the material properties of the polyamide PA2200. It was identified that laser power had greater influence on the results to increase density, flexural modulus, and stress at 10% strain obtained by the single cantilever test. Nevertheless, the scan speed also had influence, and the combination of speed and power must be taken into account to obtain the desired results.

In the case of density and flexural modulus, despite the fact that the energy density was the same, the results were different. The flexural modulus results required lower speed and power to achieve higher material stiffness. This indicates that the kinematics of the laser sintering affected the process. The time and intensity of the exposure also changed the grow rate of the necks between the polyamide particles. These effects were more pronounced when the material used was a semicrystalline polymer and it might become possible to change the spherulite sizes in microstructure, which is a direct correlation with crystallinity degree. The crystallinity directly affects the mechanical properties of the material as it reflects the way the polymer chains are structured.

## References


1. Hopkinson, N.; Hague, R. J. M.; Dickens, P. M. Rapid Manufacturing—An Industrial Revolution for the Digital Age; Wiley: New York, 2005.
2. Jacobs, P. F. Stereolithography and Other RP&M Technologies; RPA/ASME Press: New York, NY, 1996.
3. Steen, W. M. Laser Material Processing; Springer-Verlag: New York, 1991.
4. Gusarov, A. V.; Laoui, T.; Froyen, L.; Titov, V. I. Int J Heat Mass Transfer 2003, 46, 1103.
5. Gibson, I.; Shi, D. Rapid Prototyping J 1997, 3, 129.
6. Kolosov, S.; Vansteenkiste, G.; Boudeau, N.; Gelin, J. C.; Boillat, E. J Mater Process Technol 2006, 177, 348.
7. Caulfield, B.; McHugh, P. E.; Lohfeld, S. J Mater Process Technol 2007, 182, 477.
8. Hardro, P. J.; Wang, J.; Stucker, B. E. Int J Ind Eng: Theory Appl Pract 1998, 6, 203.
9. Zarringhalam, H.; Hopkinson, N.; Kamperman, N. F.; de Vlieger, J. J. Mater Sci Eng A 2006, 435, 172.
10. Ch'ng, H. N.; Pan, J. Acta Mater 2007, 55, 813.
11. EOS GmbH Electro Optical Systems. Material Data Sheet—Fine Polyamide PA2200 for EOSINT P. Available at: http://www.arptech.com.au/specs/SLS-PA2200.pdf. 2006.
12. Paggi, R. A.; Beal, V. E.; Salmoria, G. V.; Lago, A. Presented at the 19th Congress of Mechanical Engineering, COBEM, Brasilia, DF, Brazil, 2007.
13. Lu, L.; Fuh, J.; Wong, Y.-S. Laser-Induced Materials and Processes for Rapid Prototyping; Kluwer Academic Publisher: Norwell, 2001.
14. Ho, H. C. H.; Gibson, I.; Cheung, W. L. J Mater Process Technol 1999, 89/90, 204.
15. Ajoku, U.; Hopkinson, N.; Caine, M. Mater Sci Eng A 2006, 428, 211.
16. Mironov, V.; Boland, T.; Trusk, T.; Forgacs, G.; Markwald, R. R. Trends Biotechnol 2003, 21, 157.
17. Wu, B. M.; Borland, S. W.; Giordano, R. A.; Cima, L. G.; Sachs, E. M.; Cima, M. J. J Controlled Release 1996, 40, 77.